Regulation of atrial natriuretic peptide secretion by a novel Ras-like protein

Igor I. Rybkin,[1] Mi-Sung Kim,[1] Svetlana Bezprozvannaya,[1] Xiaoxia Qi,[1] James A. Richardson,[2] Craig F. Plato,[4] Joseph A. Hill,[3] Rhonda Bassel-Duby,[1] and Eric N. Olson[1]

[1]Department of Molecular Biology, [2]Department of Pathology, and [3]Department of Internal Medicine, The University of Texas Southwestern Medical Center at Dallas, Dallas, TX 75390
[4]Gilead-Colorado, Westminster, CO 80021

Atrial cardiomyocytes, neurons, and endocrine tissues secrete neurotransmitters and peptide hormones via large dense-core vesicles (LDCVs). We describe a new member of the Ras family of G-proteins, named RRP17, which is expressed specifically in cardiomyocytes, neurons, and the pancreas. RRP17 interacts with Ca^{2+}-activated protein for secretion-1 (CAPS1), one of only a few proteins known to be associated exclusively with LDCV exocytosis. Ectopic expression of RRP17 in cardiomyocytes enhances secretion of atrial natriuretic peptide (ANP), a regulator of blood pressure and natriuresis. Conversely, genetic deletion of RRP17 in mice results in dysmorphic LDCVs, impaired ANP secretion, and hypertension. These findings identify RRP17 as a component of the cellular machinery involved in regulated secretion within the heart and potential mediator of the endocrine influence of the heart on other tissues.

Introduction

Endocrine tissues and neurons release hormones and neurotransmitters through a process of regulated vesicular secretion. Abnormalities in regulated secretion cause a variety of diseases, including hypertension, diabetes, and neurological disorders. Although not widely appreciated, the heart functions as an endocrine organ by regulating blood volume and natriuresis through the secretion of natriuretic peptides (NPs) (McGrath et al., 2005). Atrial NP (ANP) is secreted exclusively by atrial myocytes, whereas brain NP (BNP) is secreted predominantly by ventricular myocytes, albeit at a low rate. In response to acute and chronic stress, ventricular myocytes up-regulate the synthesis and secretion of ANP and BNP. As such, BNP is a well-accepted clinical marker of ventricular wall stress and directly correlates with the severity of heart failure (Moe, 2005).

ANP and BNP bind to the same guanylyl cyclase-linked receptor, NP receptor-A, causing vasodilation, natriuresis, and diuresis, as well as inhibition of endothelin-1 release and the renin–angiotensin system (Silver, 2006). These effects lead to a decrease in blood volume and total peripheral resistance, thereby reducing pre- and afterload on the heart and blood pressure (Silver, 2006). BNP also prevents pathological cardiac hypertrophy and fibrosis (Tamura et al., 2000) and has emerged as a promising therapy for heart failure (Silver, 2006).

Considering their important roles in cardiovascular physiology, the stimuli that control NP synthesis have been under intense investigation over the past 30 years and extensive information has been amassed (Dietz, 2005). In contrast, the mechanisms involved in NP packaging into vesicles, trafficking of vesicles to the cardiomyocyte cell membrane, and exocytosis remain largely unexplored. In this regard, several proteins involved in vesicle formation, transport, docking, and fusion are expressed in the heart and are contained in ANP-containing LDCVs (Rossetto et al., 1996; Iida et al., 1997; Fukuda, 2003; Muth et al., 2004). However, little is known about the possible involvement of these proteins in ANP secretion.

Here, we describe a novel Ras-related protein, called RRP17, which is expressed in the heart and neuroendocrine tissues. RRP17 interacts with Ca^{2+}-activated protein for secretion-1 (CAPS1), a mediator of LDCV secretion (Walent et al., 1992), and influences the storage and secretion of ANP in cardiomyocytes in vivo and in vitro. Consistent with a possible role in regulating cardiac endocrine functions, mice lacking RRP17 display abnormalities in cardiac ANP secretion and blood pressure regulation in unconscious animals. The interaction of RRP17 with CAPS1 provides insights into the molecular basis of ANP secretion and endocrine functions of the heart.

Correspondence to Eric N. Olson: eric.olson@utsouthwestern.edu

Abbreviations used in this paper: ANP, atrial natriuretic peptide; BNP, brain natriuretic peptide; C2, calcium binding domain; CAPS1, calcium-activated protein for secretion 1; CNP, C-type natriuretic peptide; DCV, dense-core vesicle; DNP, dendroaspis natriuretic peptide; GNB, guanine nucleotide binding domain; LDCV, large dense-core vesicles; MHD, munc homology domain; NP, natriuretic peptide; PH, pleckstrin homology; RRP17, Ras-related protein 17; TAB, thoracic aortic banding.

The online version of this article contains supplemental material.

The Journal of Cell Biology, Vol. 179, No. 3, November 5, 2007 527–537
http://www.jcb.org/cgi/doi/10.1083/jcb.200707101

Results

RRP17 is a novel Ras-like protein

To identify novel signal transduction molecules involved in the regulation of cardiac function, we used microarray analysis to compare mRNA pools derived from NIH-3T3 fibroblasts and NkL-Tag cells, a mouse cardiac cell line derived from the ventricle of a transgenic mouse expressing large T antigen under control of a cardiac-specific promoter (Rybkin et al., 2003). We initially selected a pool of ESTs expressed specifically in the NkL-Tag cells and subjected these ESTs to a secondary screen through NCBI, EMBL, and Celera databases to identify uncharacterized transcripts. One EST, AA624579, belonged to the mouse UniGene cluster Mm.66275, which was classified by NCBI as encoding a novel putative Ras-like protein. Computer analysis of the mouse and human genomes revealed that the Mm.66275 cluster contains an open reading frame (ORF) encoding a putative 203-amino acid protein. The Mm.66275 transcript was confirmed by sequencing of RT-PCR products generated using heart and brain cDNAs as template. An orthologue of this protein exists in all sequenced *Coelomata* representatives including *Arthropods*, *Urochordates*, and *Echinoderms* (*Strongylocentrotus purpuratus*), but not in *Nematodes* or *Fungi*. There is high homology between orthologues of this protein, such that the mouse orthologue is 99% identical to the human protein and 67% identical to that of *Danio rerio*.

The protein encoded by the Mm.66275 UniGene cluster has a predicted secondary structure characteristic of the small G-protein superfamily and includes a guanine nucleotide-binding (GNB) domain and a prenylation signal at the C terminus, known

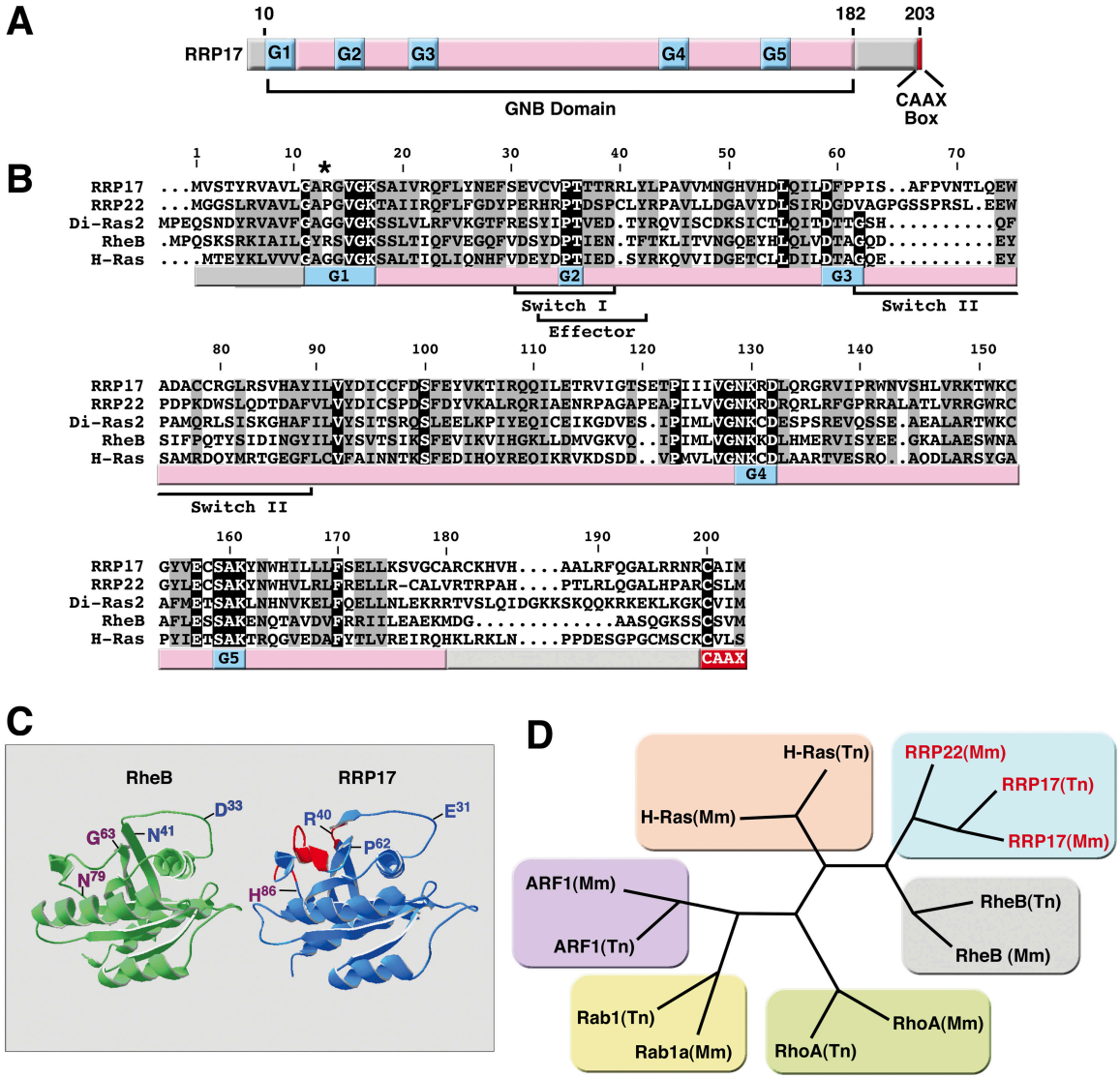

Figure 1. **Characterization of the predicted structure of RRP17.** (A) Schematic diagram of RRP17 shows a GNB (guanine nucleotide binding) domain and a CAAX box (red). Highlighted in blue are subdomains of the GNB domain (G1–G5) that bind and hydrolyze GTP. (B) Amino acid alignment of several members of the Ras superfamily (Di-Ras2, RheB, and H-Ras) with RRP17 and RRP22. Functional subdomains are identified. The R^{13} position in the G1 loop is indicated with an asterisk. (C) Crystal structure of RheB (green) (Yu et al., 2005) and predicted structure of RRP17 (blue). Highlighted in red are predicted structural differences in the Switch I (interruption of β-sheet) and Switch II (additional α-helix) regions of RRP17. (D) Dendrogram of representative mouse (*Mus musculus; Mm*) and fish (*Tetraodon nigroviridis; Tn*) members of the Ras-superfamily.

as a CAAX-box (Fig. 1 A). This putative protein is most similar to a recently described member of the small G protein superfamily Ras-related protein on human chromosome 22, RRP22 (Zucman-Rossi et al., 1996) (Fig. 1 B). Based on the nomenclature of RRP22, we named this newly identified protein RRP17 (Ras-related protein located on human chromosome 17).

Although RRP17 clearly belongs to the Ras family of small G proteins, it possesses two important features that distinguish it from other members of the Ras family. First, similar to RheB and in contrast to H-Ras, RRP17 has an arginine instead of the usual glycine at the third amino acid position of the P-loop (GA**R**GVGK(S/T)) (Fig. 1 B). The substitution of Gly (12) for a charged or bulky amino acid, such as Arg, results in a decrease of GTPase activity of Ras proteins due to steric interference with the γ-phosphate of GTP and ensures Ras oncogenicity (Krengel et al., 1990). A second difference is the 13-amino acid insertion (from D59 to E74) within the G3 loop of the Switch II region (DXXG). The glycine residue within this loop forms a hydrogen bond with the γ-phosphate of GTP, and is universally conserved through the small GTPase family (Sprang, 1997; Colicelli, 2004). In RRP17, this glycine is replaced with a hydrophobic nonflexible proline residue. RRP22 is the only other small G protein known to possess a similar size insertion that disrupts the G3 loop (see supplemental material, available at http://www.jcb.org/cgi/content/full/jcb.200707101/DC1). Although the amino acid composition of that insertion is different from the insertion of RRP17, there is a conserved proline residue within this region of both proteins, corresponding to amino acid 67 and 69 of RRP17 and RRP22, respectively. Due to this 12-amino acid insertion, the Switch II region of RRP17 is longer than the corresponding region of any known GTPase and potentially has a distinct and more rigid 3D structure compared with RheB, the closest homologue with a known crystal structure (Fig. 1 C). Indeed, 3D prediction analysis shows an additional α-helix within the Switch II region of RRP17 (Fig. 1 C). A dendrogram reveals that RRP17 and RRP22 form a distinct family within the Ras-superfamily (Fig. 1 D).

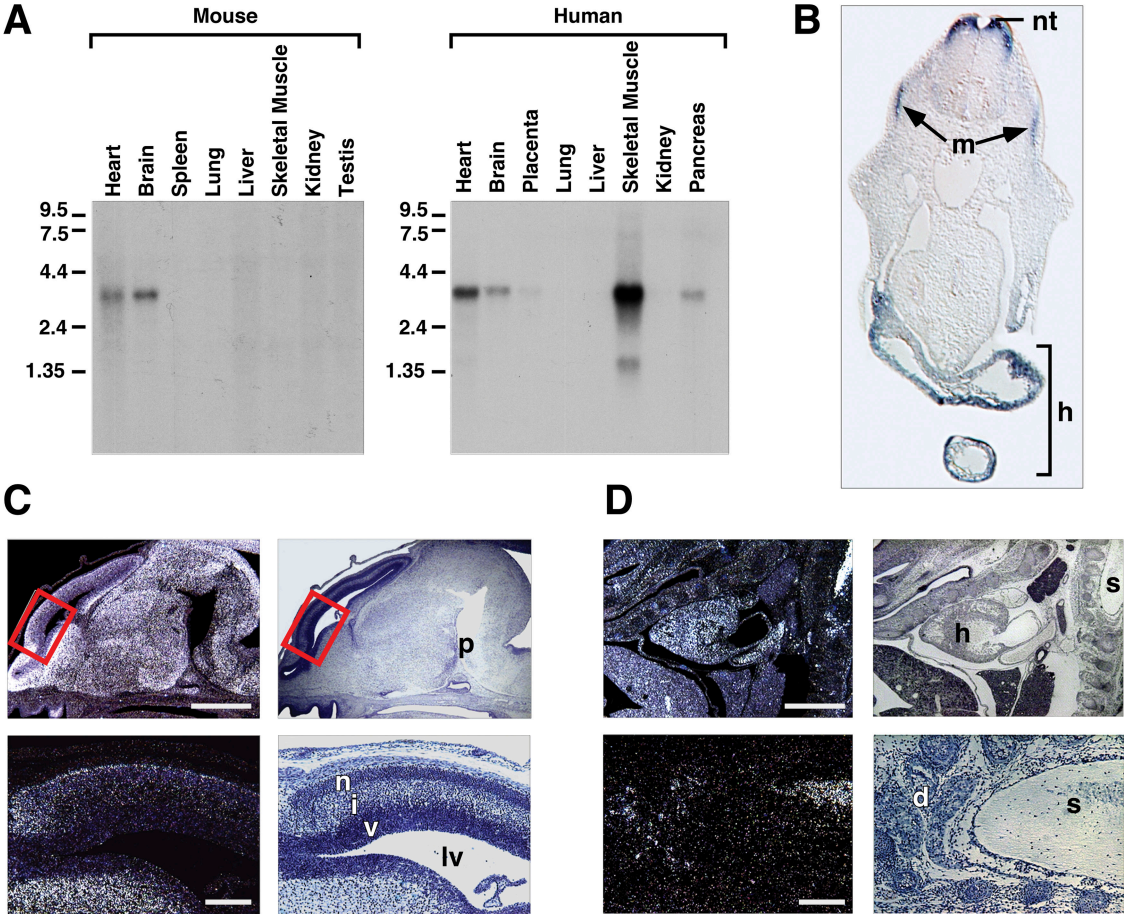

Figure 2. **Expression pattern of RRP17.** (A) Northern blot analysis of RRP17 mRNA in adult mouse and human tissues. (B) Section of an E9.5 mouse embryo after in situ hybridization with an RRP17 cDNA labeled with dig-UTP. *RRP17* transcripts are detected in the dorsal part of the neural tube (nt), skeletal myotome (m), and heart (h). (C) In situ hybridization of sections of E15.5 mouse brain. Left panels show in situ hybridization using *RRP17* cDNA labeled with ^{35}S-UTP as probe and right panels show the same sections counterstained with hematoxylin. Bottom panels show magnification of cortex area (outlined by box in top panels). *RRP17* transcript is detected in mature neurons. (n) neopalial cortex (future cerebral cortex), (i) intermediate zone; (v) ventricular zone; (lv) lateral ventricle; (p) pituitary. Bar: 500 μm for top panels, 100 μm for bottom panels. (D) In situ hybridization of sections of mouse heart and surrounding tissues at E13.5. Left panels show in situ hybridization using *RRP17* cDNA labeled with ^{35}S-UTP as probe and right panels show the same section counterstained with hematoxylin. (h) heart; (d) dorsal root ganglia, and (s) gray matter of spinal cord. Bar: 500 μm for top panels, 100 μm for bottom panels.

Expression of RRP17 in cardiac, brain, and endocrine tissues

Northern blot analysis revealed a single 3.6-kb RRP17 transcript in mouse and human heart and brain, as well as in human skeletal muscle and pancreas (Fig. 2 A). RRP17 mRNA was detected at embryonic day (E) 9.5 in the developing heart, skeletal myotomes, and dorsal portion of the neural tube by in situ hybridization (Fig. 2 B). At E13.5 and E15.5, RRP17 mRNA was detected in the heart and neural tissue including the central and peripheral nervous system. Expression of RRP17 mRNA in the embryonic brain is not uniform but restricted to more mature neurons and absent from the progenitor neuronal cells of the ventricular zone (Fig. 2 C). RRP17 mRNA is also present in mature peripheral neurons, such as the neurons of the dorsal root ganglia (Fig. 2 D) and the Auerbach's and Meissner's plexi of the intestinal tract (unpublished data). Although RRP17 expression was detected in human skeletal muscle, we did not detect it in mouse skeletal muscle, even when we examined expression in individually isolated mouse muscles, such as extensor digitorum longus, white vastus longus and soleus (unpublished data). The basis for this species-specific difference of RRP17 expression is unclear.

Interaction of RRP17 and CAPS1

In an initial effort to elucidate the functions of RRP17, we sought to identify proteins that interact with RRP17 in a yeast two-hybrid screen using brain and heart cDNA libraries and CAAX-box-deleted RRP17 as bait. 13 of the 186 positive clones encoded the C-terminal region of CAPS1, a regulator of LDCV secretion (Walent et al., 1992). CAPS1 contains several functional domains, including a C2 domain that binds calcium, a pleckstrin homology (PH) domain that binds phosphatidylinositol (4,5)-bisphosphate, a Munc homology domain (MHD) found in Munc family proteins, a family of proteins which are involved in secretion, and a dense core vesicle-binding domain (DCVD) at the C terminus (Speidel et al., 2003).

The longest cDNA identified by the yeast two-hybrid screen started immediately after the PH domain at amino acid 648 and the shortest cDNA started at amino acid 700 (Fig. 3 A). These results were confirmed by pull-down assays, which showed the association of CAPS1 with GST-RRP17 (Fig. 3 B). The specificity of interaction was demonstrated by the absence of binding of CAPS1 and GST-RhoA, a close relative of RRP17 (Fig. 3 B and Fig. 1 D), suggesting that CAPS1 does not bind every member of the Ras family. We observed that individually expressed CAPS1(670–1372) or RRP17 localized to the supernatant or pellet fraction, respectively. Therefore, we designed a cosedimentation assay which showed that coexpression of RRP17 and CAPS(670–1372) targets CAPS1 to the RRP17-containing pellet fraction (Fig. 3 C). Of note, we consistently observed that the presence of RRP17 increased the total amount of CAPS1 protein in the cell, although we do not know the mechanism of this effect.

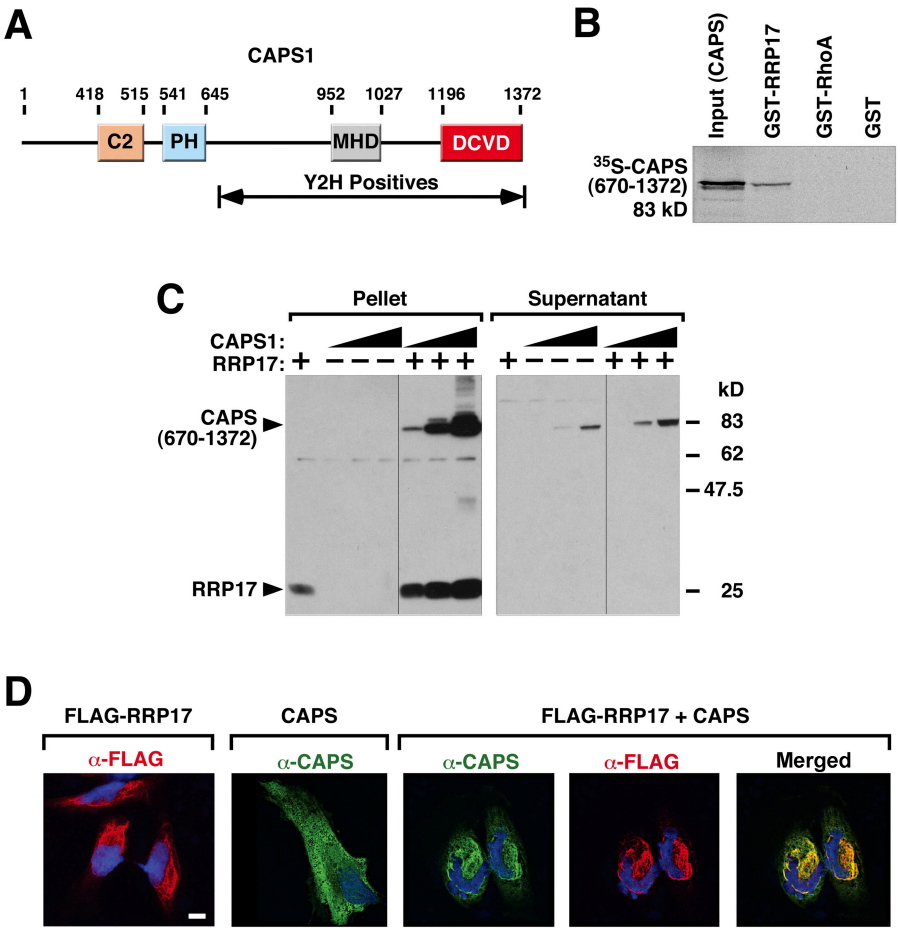

Figure 3. **Interaction of RRP17 with CAPS1.** (A) Domains of CAPS1 protein. C2, calcium binding domain; PH, plextrin homology domain; MHD, munc homology domain or DUF1041; DCVD, dense-core vesicle binding domain. Bar indicates largest yeast-two hybrid clone found in screen. (B) GST pull-down assay consisted of ^{35}S-methionine-labeled CAPS1(670–1372) incubated with GST-RRP17, GST-RhoA or GST, with glutathione Sepharose beads. Bound CAPS1(670–1372) was detected using SDS-PAGE and autoradiography. (C) COS-7 cells were transfected with Flag-RRP17 and Flag-CAPS(670–1372) expression plasmids, lysed, separated into supernatant and pellet fractions. Equal aliquots of each fraction were separated on a 10% SDS-PAGE gel and immunoblotted with anti-FLAG antibody. (D) HeLa cells were transfected with plasmids encoding full-length CAPS1 and/or Flag-RRP17. Immunohistochemistry was performed using anti-CAPS (green) and anti-Flag (red) antibodies. Nuclei were counterstained with Hoechst 33238 (blue). Cells were visualized using confocal microscopy. Bar, 10 μm.

Using immunocytochemistry, the interaction of CAPS1 and RRP17 was further confirmed in transfected HeLa cells. Exogenous RRP17 was distributed in a distinct perinuclear pattern whereas CAPS1 was distributed throughout the cytoplasm (Fig. 3 D). Upon coexpression of CAPS1 and RRP17, CAPS1 protein was redistributed to colocalize with RRP17, consistent with the interaction of the two proteins (Fig. 3 D). Residues 670–1372 of CAPS colocalized with RRP17, whereas CAPS1 deletion mutants lacking this region did not colocalize with RRP17 (unpublished data).

Up-regulation of CAPS1 expression during cardiac hypertrophy

The interaction of RRP17 with CAPS1 suggested the involvement of RRP17 in regulated secretion. The published expression pattern of mouse CAPS1 is similar to that of RRP17, except that CAPS1 was not previously detected in heart (Walent et al., 1992). Given that the normal adult heart secretes NPs only from the atria, we isolated RNA from the cardiac atria and ventricles independently and analyzed CAPS1 expression. CAPS1 mRNA was detected in atrial, but not ventricular RNA (Fig. 4 A).

We speculated that if CAPS1 participated in the secretion of cardiac NPs, then it should be expressed in ventricular cardiomyocytes during conditions that enhance NP secretion. To test this hypothesis, we analyzed ventricular myocytes from two different mouse models of cardiac hypertrophy; using the α-MHC-CnA transgenic mouse line that overexpresses activated calcineurin in the heart (Molkentin et al., 1998) and surgical partial occlusion of the thoracic aorta (TAB) (Hill et al., 2000).

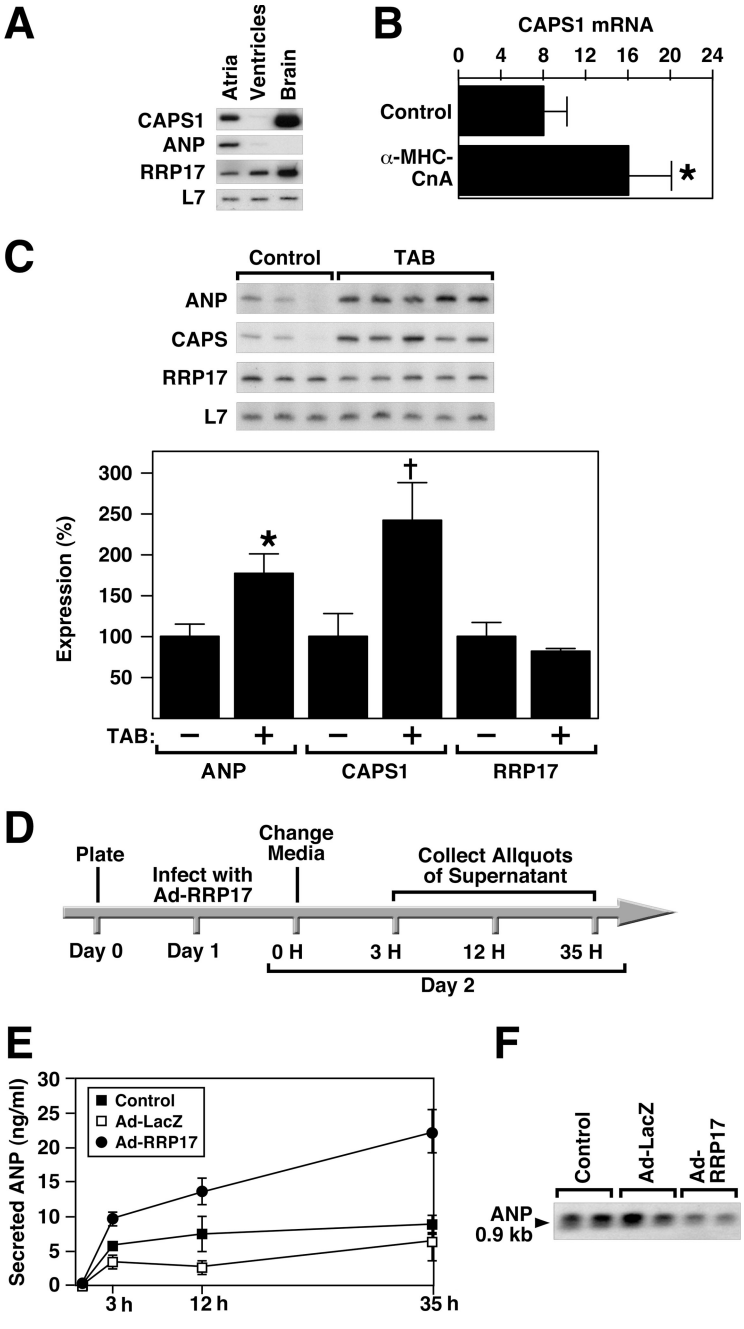

Figure 4. **Expression of RRP17 in cardiomyocytes enhances secretion of ANP.** (A) RT-PCR of heart atria, heart ventricles, and brain RNA was performed in the presence of ^{32}P-α-dCTP using primers for CAPS1, ANP, and RRP17 transcripts. RT-PCR products were normalized to L7, separated on 8% acrylamide gels and visualized with a PhosphorImager. (B) RT-PCR of heart ventricle RNA isolated from wild-type (control) and α-MHC-CnA mice was performed in the presence of ^{32}P-α-dCTP using primers for CAPS1 transcript. RT-PCR products were normalized to L7, separated on 8% acrylamide gels, visualized and quantified with a PhosphorImager. (*t* test; *, $P < 0.05$; $n = 3$; error bars show SD). (C) RT-PCR of heart ventricle RNA isolated from wild-type mice (control) and mice subjected to thoracic aorta occlusion (TAB). RT-PCR was performed in the presence of ^{32}P-α-dCTP using primers for ANP, CAPS1, and RRP17 transcripts. RT-PCR products were normalized to L7 product, separated on 8% acrylamide gels, visualized and quantified with a PhosphorImager. (One-way ANOVA; *, $P < 0.05$ difference of ANP expression between control and TAB; †, $P < 0.05$ difference of CAPS expression between control and TAB). (D) Time-line of ANP secretion study. Primary neonatal rat ventricular myocytes were infected with recombinant adenovirus expressing RRP17 (Ad-RRP17) or β -galactosidase (Ad-lacZ) on Day 1. Media was changed on Day 2 and aliquots were collected as indicated. (E) Secreted ANP was measured in the media from primary rat cardiomyocytes infected with adenovirus expressing RRP17 (Ad-RRP17), β-galactosidase (Ad-lacZ), or uninfected (control) at 3, 12, and 35 h post-infection. (Two-way ANOVA, $P < 0.05$; $n = 4$; error bars show SD). (F) ANP mRNA was determined by Northern blot analysis in cardiomyocytes infected with adenovirus expressing RRP17 (Ad-RRP17), β-galactosidase (Ad-LacZ) or uninfected (control) at 35 h after infection.

Indeed, the level of CAPS1 mRNA was significantly increased in the ventricles of mice with calcineurin-induced cardiac hypertrophy (Fig. 4 B). Similarly, cardiac hypertrophy induced by increased afterload due to thoracic aorta banding (TAB) caused substantial up-regulation of CAPS1 mRNA in parallel with ANP mRNA (Fig. 4 C). These findings show that CAPS1 and RRP17 are coexpressed in the atria and that expression of CAPS1 mRNA in the ventricles is augmented by hypertrophic stimuli, suggesting that RRP17 and CAPS1 may participate in regulated secretion of NPs in hypertrophic ventricular myocytes. Interestingly, the expression level of RRP17 mRNA was unaffected by these hypertrophic stimulus (Fig. 4 C, and unpublished data).

RRP17 promotes secretion of ANP in primary rat cardiomyocytes

To further explore the potential involvement of RRP17 in NP secretion, we infected primary rat neonatal cardiomyocytes with recombinant adenovirus expressing either Flag-RRP17 protein or β-galactosidase as a control. 16 h after infection, medium supplemented with serum was replaced with serum-free medium

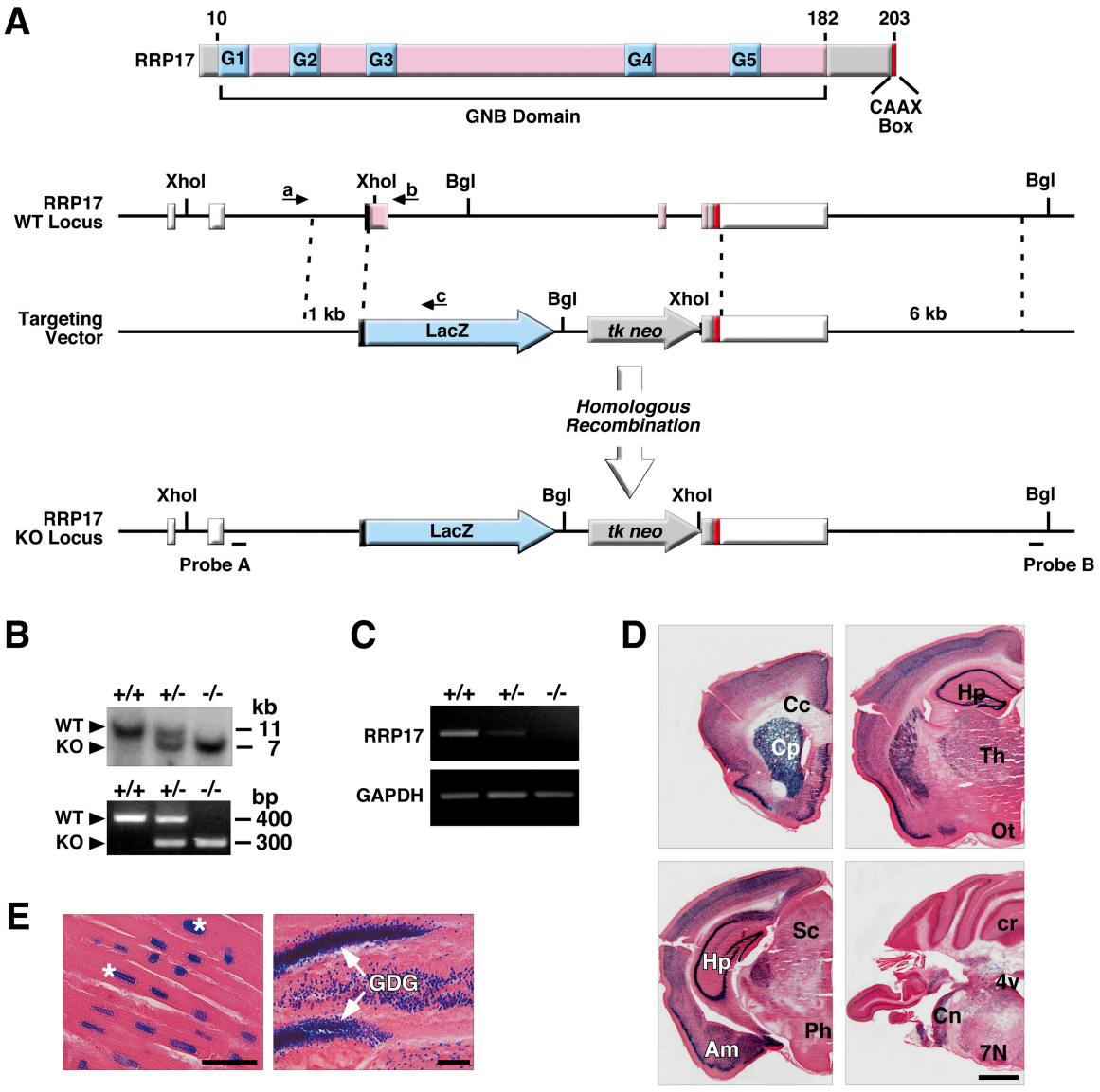

Figure 5. **Generation of RRP17$^{-/-}$ mice.** (A) Mouse RRP17 protein is schematized on top of the *RRP17* genomic loci showing five exons with the first two exons being alternatively spliced. The targeting vector, which contains a 1 kb 5′ arm and a 6 kb 3′ arm, replaced a 6 kb region of the gene with a lacZ-neo cassette deleting the entire ORF encoded by exons 2, 3, and part of exon 4. White boxes mark the 5′ and 3′ UTR. Probe A and Probe B were used in Southern blot genotyping. Primers a, b, and c were used in PCR genotyping. (B) Southern blot analysis of genomic DNA isolated from *RRP17* knockout mice using the probe B after digestion with Bgl II (top). PCR analysis of the short arm recombination (bottom) using primers a, b, and c. (C) RT-PCR of RRP17 transcript from heart RNA isolated from wild-type (+/+), heterozygote (+/−), and homozygote (−/−) mice of the *RRP17* allele. GAPDH is used as control. (D) Coronal sections of adult RRP17$^{+/-}$ mouse brain stained for lacZ activity and counterstained with eosin. (Cp), caudate putamen; (Cc), corpus colosum; (Hp), hippocampus; (Th), thalamus; (Ot) optical tract; (Am), amygdala; (Sc), superior colliculus; (Ph), posterior hypothalamus; (Cr), cerebellum; (4v), fourth ventricle; (7N), facial nucleus; (Cn), cochlear nucleus. Bar, 1 mm. (E) Sections of adult RRP17$^{+/-}$ mouse heart (left) and hippocampus (right) were stained for lacZ activity and counterstained with eosin. (GDG) granular level of dental gyrus. Bars: 40 μm (left) and 100 μm (right).

and the amount of secreted ANP was measured 3, 12, and 35 h later (Fig. 4 D). Cardiomyocytes infected with adenovirus expressing RRP17 secreted 2.5- and 3.5-fold more ANP compared with uninfected or lacZ expressing cardiomyocytes, respectively (Fig. 4 E). The enhancement of ANP secretion by RRP17 was not associated with an elevation of ANP mRNA expression (Fig. 4 F). These results suggest that RRP17 facilitates release of ANP in cardiomyocytes.

Generation of RRP17 knockout mice

To determine the function of RRP17 in vivo, we generated RRP17-deficient mice by targeted disruption of the *RRP17* gene. The mouse *RRP17* gene spans ≈12 kb on chromosome 11 and consists of three protein-coding exons and two alternative exons in the 5′ untranslated region (UTR) (Fig. 5 A). The ORF starts within exon 2 and is not affected by alternative splicing of the 5′ UTR. To generate mice lacking RRP17, exon 3 and portions of exons 2 and 4 were replaced with a promoterless nuclear LacZ gene and a neomycin-resistance gene such that the targeted allele lacked almost the entire RRP17 ORF (Fig. 5 A). The targeting vector was electroporated into 129SV/Ev ES cells and targeted clones were identified by Southern blot analysis of genomic DNA (Fig. 5 B). Embryonic stem cells heterozygous for the RRP17 deletion were injected into C57BL/6 blastocysts, and chimeric mice transmitted the mutant allele through the germ line.

Mice homozygous for the mutant *RRP17* allele were viable and fertile and were obtained in Mendelian ratios from $RRP17^{+/-}$ intercrosses. There was no obvious phenotype observed in null animals when left undisturbed. RT-PCR analysis of heart and brain RNA showed diminished expression of the RRP17 transcript in heterozygous mice and its complete absence in homozygous mutant mice (Fig. 5 C, and unpublished data).

The expression pattern of β-galactosidase from the mutant allele recapitulated the pattern of *RRP17* mRNA expression in the central nervous system and heart (Fig. 5, D and E). In adult brain, the expression of β-galactosidase from the *RRP17* locus was restricted to neurons of the cortex, hippocampus, and cerebellum, but was sparse in the brainstem and almost absent in the hypothalamic region (Fig. 5 D). The expression of nuclear lacZ from the *RRP17* gene was confined to neurons and cardiomyocytes and not detected in interstitial tissue or vascular cells (Fig. 5 E).

Storage and secretion defect of ANP in $RRP17^{-/-}$ mice

Consistent with the involvement of RRP17 in vesicular secretion, electron microscopy of atria of wild-type and $RRP17^{-/-}$ mice showed that LDCVs were smaller in the mutant than in wild-type cardiomyocytes (Fig. 6 A), although the difference in the mean of the vesicle size did not reach statistical significance (unpublished data). Passive stretch, the major stimulus for ANP secretion in the heart (Ruskoaho et al., 1997), can be simulated in cell culture by challenging isolated cardiomyocytes with hypotonic buffers. A decrease in the extracellular osmolarity from 300 to 200 mOsm/kg H_2O causes an increase in cardiomyocyte volume by 50% and induces secretion of prestored ANP granules (Roos, 1986; Greenwald et al., 1989; Jiao et al., 2000). Normally, passive mechanical stretch causes prompt translocation of LDCVs from the perinuclear area of atrial cardiomyocytes toward the cellular membrane (Agnoletti et al., 1989).

Challenging atrial cardiomyocytes isolated from wild-type mice with hypotonic buffer resulted in secretion of 50 to 60% of stored ANP during the first 10 min, with no appreciable secretion of ANP for the next 50 min (Fig. 6 B). RRP17-deficient myocytes also responded within the first 10 min; however, they secreted only 10 to 20% of stored ANP (Fig. 6 B).

Hemodynamic measurements showed that the anesthetized $RRP17^{-/-}$ mice displayed a significantly higher systolic and diastolic blood pressure, reflected in the mean arterial pressure, and a higher heart rate (Fig. 6 C). Consistent with their impaired ability to secrete ANP, the amount of ANP in the atria was significantly higher in $RRP17^{-/-}$ mice compared with wild-type mice (Fig. 6 D).

Discussion

LDCVs mediate secretion of many biologically active substances from cardiomyocytes, neurons, and endocrine cells. Small GTPases are known to be involved in regulation of multiple steps of LDCV secretion with functions ranging from vesicle formation to vesicle transport, tethering to the cellular membrane and fusion steps (Burgoyne and Morgan, 2003; Aizawa and Komatsu, 2005). In this study, we describe a previously unknown Ras-like protein, RRP17, which regulates secretion of ANP from cardiomyocytes and interacts with CAPS1, a protein involved in biogenesis and storage of LDCV.

Classification of members of the Ras superfamily is based on similarity of amino acid sequence (Wennerberg et al., 2005). At a level of identity of 30%, five major Ras families have been identified, Ras, Rho, Arf, Ran, and Rab. RRP17 and RRP22 proteins differ from other members of the Ras-superfamily within the Switch I and II regions, which bind and hydrolyze GTP and interact with regulators and effectors of G protein signaling (Sprang, 1997). The glycine residue of the Switch II region, which coordinates the positioning of Mg^{2+} ion and γ-phosphate of GTP, is substituted by a proline residue in RRP17. In addition, the Switch II region of RRP17, predicted to adopt an α-helix structure, is 12 amino acids longer than the corresponding region of other members of the Ras superfamily (Sprang, 1997). These differences suggest that RRP17 utilizes a distinct mechanism of coordination and hydrolysis of GTP, and imply that RRP17 interacts with a unique set of effectors and regulators.

RRP17 binds to CAPS1, a MUN domain protein involved in biogenesis and storage of LDCVs in neuronal and endocrine cells (Basu et al., 2005; Speidel et al., 2005). Interestingly, Munc13-4, another MUN domain–containing protein, interacts with Rab27 to regulate dense core granule secretion in platelets (Shirakawa et al., 2004). Although the exact domain of Munc13-4 that binds Rab27 has not been identified, the RRP17-interacting domain of CAPS1 spans most of the sequence between the PH and DCVD domains (unpublished data) and roughly corresponds to the MUN domain of the Munc13 protein (Basu et al., 2005).

The MUN domains of Munc13 (Basu et al., 2005) and CAPS1 (unpublished data) have a predicted tertiary structure

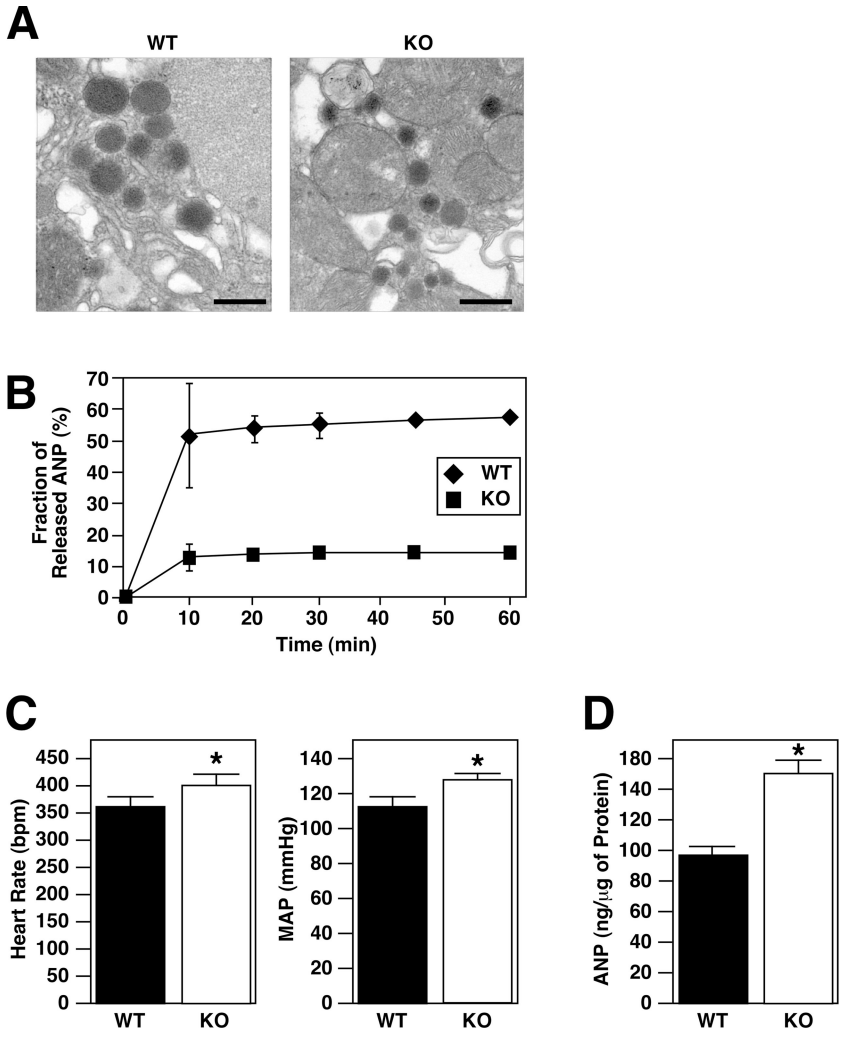

Figure 6. **Cardiac phenotype of RRP17$^{-/-}$ mice.** (A) Electron microscopy of atrial cardiomyocytes from wild-type (WT) and *RRP17*$^{-/-}$ (KO) mice. Asterisk denotes large dense-core vesicle (LDCV) containing ANP. Bar, 500 nm. (B) Atrial cardiomyocytes isolated from wild-type (WT) or *RRP17*$^{-/-}$ (KO) were subjected to stretch using hypotonic buffer. Media was collected at various time-points after stretch. The amount of ANP secreted into the medium was measured using RIA and expressed as a fraction of the total amount of ANP in the medium and cells. Data are expressed as means ± SE (two-way ANOVA, $P < 0.05$; $n = 6$; error bars show SD). (C) The carotid arteries of isoflurane-anesthetized wild-type (WT) and *RRP17*$^{-/-}$ (KO) mice were catheterized and the heart rate (left) and mean arterial blood pressure (MAP) (right) were directly measured (*t* test; *, $P < 0.05$; $n = 7$ for WT and $n = 9$ for KO; error bars show SD). (D) ANP was measured in the atria of wild-type (WT) and *RRP17*$^{-/-}$ (KO) mice (*t* test; *, $P < 0.05$; $n = 7$ for WT and $n = 9$ for KO; error bars show SD).

similar to that of importin β. Of note, importin β interacts with Ran GTPase through three binding regions, Switch I, Switch II, and the C-terminal α-helix. Co-crystallization of importin β and Ran-GTPase showed that importin β forms a right-handed superhelix that serves as a binding pocket for RanGTP (Lee et al., 2005). Based on structural analysis, RanGTP has been proposed to insert itself into a cylinder formed by the importin β superhelix, thereby discharging importin β's cargo. Further studies are needed to determine whether RRP17 interacts with CAPS1 in a similar fashion.

We show that RRP17 is expressed in atria and ventricles of mice, whereas CAPS1 is present only in the atria. However, upon induction of cardiac hypertrophy, CAPS1 appears in ventricular myocytes. This finding suggests that ventricular myocytes may use the regulated secretion pathway during hypertrophy. It is known that atrial and ventricular myocytes secrete ANP and BNP via the regulated and constitutive secretion pathways, respectively (Bloch et al., 1986). However, several reports suggest that ventricular myocytes concurrently display constitutive and regulated secretion pathways (Irons et al., 1993). Our findings suggest that during cardiac hypertrophy ventricular myocytes activate the regulated secretion pathway, in addition to the constitutive secretion pathway.

Although our results demonstrate a clear role for RRP17 in LDCV secretion, we acknowledge that RRP17 is also expressed in tissues that do not possess LDCV secretion (e.g., skeletal muscle). These findings suggest that RRP17 may have additional functions yet to be determined.

Overexpression of RRP17 in cardiac myocytes enhances secretion of ANP, whereas loss-of-function studies showed that hypertonic-stretched atrial myocytes isolated from *RRP17*$^{-/-}$ mice were defective in ANP release. The exact mechanism of the decrease of ANP secretion in *RRP17*$^{-/-}$ mice is not entirely clear and may be explained by a reduced rate of secretion or a packaging defect. Consistent with these findings, electron microscopy showed smaller than normal LDCVs in *RRP17*$^{-/-}$ atrial myocytes. Notably, deletion of one allele of CAPS1 also results in perturbation of LDCV intracellular distribution (Speidel et al., 2005), which may reflect a defect in vesicle trafficking (Sudhof, 2005).

ANP plays an important role in regulation of blood pressure via direct action on renal function and the peripheral vasculature, as well as via inhibition of the renin–angiotensin system and suppression of release of endothelin-1 (Silver, 2006). Therefore, dysregulation of ANP release may cause elevation of blood pressure, as seen in mice lacking the ANP receptor

(Lopez et al., 1995). Deletion of RRP17 in mice increased atrial ANP content and was associated with arterial hypertension and tachycardia in anesthetized mice. Of note, the elevation of mean arterial blood pressure in unconscious *RRP17*$^{-/-}$ mice is in the same range as seen in the *ANP*$^{-/-}$ mice (Melo et al., 1998). However, the pathophysiological basis of the elevation of blood pressure in *RRP17*$^{-/-}$ mice is, in all likelihood, more complex than in *ANP*$^{-/-}$ mice due to expression of RRP17 in other endocrine organs and the central nervous system.

The discovery of RRP17 and its role in the secretion of cardiac NPs provides new insights into the molecular mechanisms underlying the endocrine influences of the heart and may ultimately contribute to an understanding of the pathophysiology of cardiovascular diseases as well as the molecular basis of unresolved heterogeneity of BNP levels among different individuals with heart failure.

Materials and methods

cDNA and bioinformatics

EST (AA624579), obtained previously by microarray analysis (Rybkin et al., 2003), was analyzed using the NCBI BLAST server. This EST, shown to belong to the UniGene Mm.66275 cluster, was designated as a putative novel Ras-like protein-10B, Rasl10B. The complete cDNA of the *RRP17* gene was constructed by alignment of partial human and mouse cDNAs and ESTs deposited in NCBI, followed by RT-PCR verification. The structure of the *RRP17* gene was determined via alignment of cDNA sequences (three splice variants of *RRP17* cDNA were observed) to the mouse and human genomes in the NCBI database followed by human to mouse comparison using VISTA server (http://genome.lbl.gov/vista/index.shtml).

The prediction of the secondary structure of RRP17 protein and alignment to other Ras-like proteins were performed using ClustalW Alignment Algorithm on MacVector 6.5.3 software, and PBIL server (http://pbil.univ-lyon1.fr). A phylogenetic tree was constructed using Cluster and Topological algorithms via GeneBee Database Service (http://www.genebee.msu.su/genebee.html). Three-dimensional prediction and alignment of RRP17 to small G proteins of determined crystal structure were performed using 3D-PSSM (http://www.sbg.bio.ic.ac.uk/~3dpssm), Cn3D 4.1 software (NCBI), and DeepView/Swiss-Pdb Viewer software (GlaxoSmithKline).

Northern blot analysis and RT-PCR

Isolation of RNA from brain, heart, skeletal muscle, and cells for Northern blot analysis and RT-PCR was performed using TRIzol according to the manufacturer's protocol (Invitrogen). Human and mouse multiple tissue Northern blots were purchased from CLONTECH Laboratories, Inc. DNA probes to detect human or mouse RRP17 transcripts were derived from heart cDNA using species-specific primers.

For semi-quantitative PCR, cDNA was generated from 2 μg of total RNA with random-hexamer primers using the Superscript III kit (Invitrogen). To perform semi-quantitative PCR, 0.1 μl of ^{32}P-dCTP (10 μCi/μl) was added per 25-μl reaction and the PCR product was resolved on an acrylamide gel. The radioactive signal was detected and quantified using a PhosphorImager (GE Healthcare) and X-ray film (Kodak). To ensure that equal amounts of cDNA were added to each reaction sample, L7 primers were initially used to determine the amount of cDNA per sample. Amplifications with L7 primers were performed at different numbers of cycles to ensure that densitometry was performed within linear range. Based on these results, calibrated amounts of cDNA were used in the PCR reactions. Primer sequences are available upon request.

In situ hybridization and lacZ staining

Mouse embryos at ages ranging from E7.5 to E15.5 were dissected and fixed in 4% paraformaldehyde in PBS treated with diethylpyrocarbonate. Whole-mount and section in situ hybridizations were performed as described previously (Nakagawa et al., 1999), using sense and antisense probes prepared from RRP17 cDNA. Images of whole-mount in situ hybridization were captured by a microscope (M420; Leica) using a 3CCD camera (C5810; Hamamatsu). Images of radioactive in situ hybridization were captured using a microscope (DM2000; Leica) with a camera (VI470; Optronic) using 2.5× and 10× objectives. Images were processed using Adobe Photoshop 7.0.

LacZ staining was performed on heart and brain sections of adult mice using β-gal staining solution (5 mM potassium ferrocyanide, 5 mM potassium ferricyanide, 2 mM Mg_2Cl, and 1 mg/ml X-gal in PBS) overnight at room temperature. Images were captured on a Stemi SV11 microscope (Carl Zeiss MicroImaging, Inc.) with Apochromatic optics and a Macrofair camera (Optronics) (Fig. 5 C) and a DM2000 microscope (Leica) with VI470 camera (Optronics) (Fig. 5 D) using 10× and 40× objectives. Captured images were exported as 8-bit TIFF files and processed using Adobe Photoshop 7.0.

Generation of constructs

RRP17 expression constructs were generated by PCR-based cloning using mouse RRP17 cDNA as a template and were subcloned into pcDNA3 vectors (Invitrogen) with N-terminal Flag tag. Full-length rat HA-CAPS1 was provided by Thomas F.J. Martin (University of Wisconsin). C-terminal fragments of CAPS1 (amino acid residues are indicated in the results section) were generated by PCR using the Y2H prey as a template. All PCR products were verified by sequencing.

Yeast two-hybrid screen

To generate "bait" for a yeast two-hybrid screen, the *RRP17* wild-type cDNA lacking the sequence encoding the CAAX box was subcloned into pGBKT7 vector (CLONTECH Laboratories, Inc.) in frame with the GAL4 DNA-binding domain at the C-terminus. The CAAX box of RRP17 was omitted from the fusion protein to prevent targeting of the protein to the cellular membrane due to prenylation. Adult heart and brain cDNA libraries, subcloned into pACT2 vector, were fused to the C terminus of the GAL4 trans-activation domain (CLONTECH Laboratories, Inc.). The "bait" was cotransfected with the indicated cDNA library into AH109 yeast cells and the assay was performed according to the MATCHMAKER GAL4 Two-Hybrid System 3 protocol (CLONTECH Laboratories, Inc.).

GST protein binding assay

GST-tagged RRP17 cDNA was subcloned into pGEX-KG vector (GE Healthcare) and expressed in BL21(LysS) *Escherichia coli* grown in LB supplemented with 0.5 M sorbitol and 2.5 mM betaine. Protein expression was induced by the addition of 250 mM isopropylthio-β-D-galactoside (IPTG) for 4 h at room temperature. Protein purification was performed according to published protocols with some modifications (Novagen Manual).

CAPS1 protein was in vitro translated using TNT kit (Promega) in the presence of ^{35}S-methionine followed by incubation with equal amounts of recombinant GST-RRP17, GST-RhoA, or GST in 50 mM Hepes-KOH (pH 7.4), 100 mM NaCl, 1.5 mM $MgCl_2$, 0.1% NP-40, 10 μM GDP, and complete EDTA-free protease inhibitors (Roche) for 1 h at 4°C. Concentrations of recombinant proteins were estimated on SDS-PAGE using serial dilutions. Glutathione Sepharose (GE Healthcare) was added and incubated for 15 min followed by four washes with centrifugation at 2,000 *g*. The pellet resulting from the final wash was boiled in SDS-loading buffer and resolved on a 4–15% gradient SDS-PAGE gel. The gels were dried and exposed to X-ray film for autoradiography.

Cell culture and transfection

Cells (HeLa and COS-7) were cultured in DME supplemented with 10% FBS, L-glutamine, and penicillin/streptomycin at 37°C. Cell transfections were performed using FuGene6 reagent (Roche) according to the manufacturer's instructions.

Rat neonatal cardiomyocytes were isolated and infected with recombinant adenovirus as previously described (Song et al., 2006). Samples of media were collected at indicated intervals and processed by radioimmunoassay (RIA). At the end of the experiment, one half of plates were used for protein isolation and other half for RNA isolation to determine the level of ANP peptide and mRNA, respectively.

Generation of recombinant adenovirus and infection

Recombinant adenovirus expressing full-length RRP17, and β-galactosidase proteins were generated using a Cre-loxP in vitro recombination system as previously described (Rybkin et al., 2003). Cardiomyocytes were infected at a multiplicity of infection (MOI) of 10 for 3 h in plating medium, after which the medium was replaced with fresh growth medium.

Radioimmunoassay (RIA) for ANP

The amount of ANP secreted into the cell culture media of primary neonatal cardiomyocytes was measured using a commercially available ANP RIA kit (Peninsula Labs) according to the manufacturer's instructions. Collected

media was titered to ensure that the radioactive counts were within the slope of the standard curve. Each sample was measured in duplicate.

To measure ANP in atria, isolated atria were snap frozen in liquid nitrogen, weighed, and homogenized in 10× volume of 0.1 M CH_3COOH using a Dounce homogenizer. Homogenates were centrifuged at 30,000 *g* for 30 min at 40°C. Supernatants were stored at −80°C until processed by RIA. Each sample was measured in duplicate.

To measure ANP in plasma, whole blood samples were collected via direct cardiac puncture on 3.8% EDTA (9:1 blood/EDTA) and aprotinin (50 KIU/μl). Blood samples were kept on ice until the completion of the study and then centrifuged at 1,000 *g* for 10 min at 4°C. Plasma was then removed and then snap frozen in liquid nitrogen.

Immunocytochemistry

Cells were fixed for 10 min with either −20°C methanol or 4% paraformaldehyde, blocked with 10% normal goat serum (NGS) in PBS containing 0.1% Triton X-100 for 30 min followed by incubation with primary antibodies in 5% NGS/PBS for 1 h at room temperature. Working dilutions of primary antibodies used were as follows: polyclonal anti-Flag (1:300; Sigma-Aldrich), and monoclonal anti-CAPS (1:100; BD Transduction Laboratories). The cells were washed three times with 0.1% Triton X-100/PBS before the addition of secondary antibodies conjugated to either FITC or Cy3 (1:400, Jackson ImmunoResearch Laboratories) and counterstained with Hoechst 33238. Coverslips were mounted on glass slides using Vectashield (Vector Laboratories). Images were captured on a confocal laser scanning microscope with 63× oil immersion objective lens (model LSM 510-V3.2; Carl Zeiss MicroImaging, Inc). Captured images were exported as 8-bit TIFF files and processed using Adobe Photoshop 7.0.

Gene targeting

An *RRP17* targeting vector was constructed to delete most of the coding region, including the starting ATG codon, by using a pN-Z-TK2 vector (a gift of R. Palmiter, University of Washington, Seattle, WA). The targeting vector contains a nuclear *LacZ* (*nLacZ*) cassette and a *neomycin resistance* gene under the control of the RNA polymerase II promoter flanked by cloning sites and *thymidine kinase* (*TK*) gene cassettes. Both arms of the targeting vector were obtained by PCR from a mouse 129SvEv genomic library using High Fidelity PCR kit (Roche), sequenced and verified against the NCBI database. The short arm comprises sequences from 1009 to 80 bp upstream of the first ATG codon. The long arm comprises sequences starting from the nucleotide coding amino acid 145 and continuing 6 kb downstream. The targeting vector was electroporated into 129SvEv-derived ES cells, and targeted cells were selected with G-418 and FIAU. 500 ES clones were isolated and analyzed by Southern blot analysis for homologous recombination. Three targeted clones were injected into 3.5-d C57BL/6 mouse blastocysts. The resulting chimeric mice were bred to C57BL/6 females to achieve germline transmission of the mutant allele. Only mice of the 129SV/Ev × C57Bl6 mixed background were characterized in this study.

Hypotonic stress of primary mouse cardiomyocytes

Primary atrial cardiomyocytes were isolated essentially as described for rat neonatal cardiomyocytes, with some modifications. In brief, the left and right atria from 10 to 15, 2–4 day-old mice were isolated under a dissection scope. Dissected tissues were minced and digested with 0.08% Collagenase Type II and 0.025% DNase Type I (Worthington). Cells were plated onto 24-well Primaria plates (Fisher Scientific) with fresh DMEM/F12 medium containing 5% horse serum (measured osmolarity ~315 mOsm/kgH_2O) being replaced the next day. The cells were used 2 d after isolation. The medium was replaced with hypotonic buffer (100 mM NaCl, 5 mM KCl, 1 mM $CaCl_2$, 1.5 mM $MgCl_2$, 10 mM glucose, and 10 mM Hepes-NaOH, pH 7.3) at time "0" followed by 10-, 20-, 30-, and 60-min time points. Osmolarity of buffer (~232 mOsm/kgH_2O) was confirmed by freezing-point depression osmometry using a Fiske Micro-Osmometer Model 210. All fractions were collected into siliconized Eppendorf tubes for further analysis by RIA. Cells remaining on the plates were harvested into hypotonic buffer (as above), freeze-opened, and used for ANP RIA and DNA content estimation (for normalization). To estimate the amount of DNA in each well, aliquots of cell lysates were mixed with 0.1 mg/ml Hoechst 33238 solution at a 1:4 ratio and the samples were analyzed using a FLUOstar Optima plate reader (excitation at 365 nm, emission at 458 nm). The amount of ANP secreted into the medium was expressed as a fraction of the total amount of ANP in the medium and cells. Data are expressed as means ± SE, with each experiment (consisting of 5–6 samples) being presented as an individual line on the graph.

Thoracic aortic banding

To induce left ventricular hypertrophy, 6-wk-old mice were subjected to either thoracotomy (sham) or thoracotomy with partial occlusion of transverse aortic arch using a 27-gauge needle as previously described (Hill et al., 2000).

Hemodynamic measurements

To measure systemic hemodynamics, mice were anesthetized via isoflurane inhalation and transferred to a heat-controlled pad to maintain constant body temperature. The right carotid artery was exposed via direct midline neck incision, the distal end ligated, and the proximal end of the artery was catheterized with 1.4F Millar catheter (Millar Instruments). After allowing the animal a minimum of 30 min for stabilization, a minimum of 15 min of steady-state data were obtained.

Online supplemental material

The supplement shows the multiple alignment of GTP binding domains of representatives of the Ras family. The blue box highlights members of the RRP17 family. Online supplemental material is available at http://www.jcb.org/cgi/content/full/jcb.200707101/DC1.

We thank April Hawkins and Kristin M. Joly for technical assistance; Dr. Robert Gerard for help with adenovirus production; John Shelton for assistance with in situ hybridization; Alisha Tizenor and Angela Diehl for graphics; Dr. Thomas F.J. Martin for providing rat HA-CAPS1 construct; and Drs. Steven Sprang, Nick Grishin, and the members of the Olson lab for helpful discussion.

This work was supported by grants from the National Institutes of Health, the Donald W. Reynolds Center for Cardiovascular Clinical Research, and the Robert A. Welch Foundation to E.N. Olson. I.I. Rybkin was supported by NIH Kirschstein-NRSA fellowship.

Submitted: 13 July 2007
Accepted: 1 October 2007

References

Agnoletti, G., R. Ferrari, A.M. Slade, N.J. Severs, and P. Harris. 1989. Stretch-induced centrifugal movement of atrial specific granules–a preparatory step in atrial natriuretic peptide secretion. *J. Mol. Cell. Cardiol.* 21:235–239.

Aizawa, T., and M. Komatsu. 2005. Rab27a: a new face in beta cell metabolism-secretion coupling. *J. Clin. Invest.* 115:227–230.

Basu, J., N. Shen, I. Dulubova, J. Lu, R. Guan, O. Guryev, N.V. Grishin, C. Rosenmund, and J. Rizo. 2005. A minimal domain responsible for Munc13 activity. *Nat. Struct. Mol. Biol.* 12:1017–1018.

Bloch, K.D., J.G. Seidman, J.D. Naftilan, J.T. Fallon, and C.E. Seidman. 1986. Neonatal atria and ventricles secrete atrial natriuretic factor via tissue-specific secretory pathways. *Cell.* 47:695–702.

Burgoyne, R.D., and A. Morgan. 2003. Secretory granule exocytosis. *Physiol. Rev.* 83:581–632.

Colicelli, J. 2004. Human RAS superfamily proteins and related GTPases. *Sci. STKE.* 2004:RE13.

Dietz, J.R. 2005. Mechanisms of atrial natriuretic peptide secretion from the atrium. *Cardiovasc. Res.* 68:8–17.

Fukuda, M. 2003. Molecular cloning, expression, and characterization of a novel class of synaptotagmin (Syt XIV) conserved from *Drosophila* to humans. *J. Biochem. (Tokyo).* 133:641–649.

Greenwald, J.E., M. Apkon, K.A. Hruska, and P. Needleman. 1989. Stretch-induced atriopeptin secretion in the isolated rat myocyte and its negative modulation by calcium. *J. Clin. Invest.* 83:1061–1065.

Hill, J.A., M. Karimi, W. Kutschke, R.L. Davisson, K. Zimmerman, Z. Wang, R.E. Kerber, and R.M. Weiss. 2000. Cardiac hypertrophy is not a required compensatory response to short-term pressure overload. *Circulation.* 101:2863–2869.

Iida, H., S. Tanaka, and Y. Shibata. 1997. Small GTP-binding protein, Rab6, is associated with secretory granules in atrial myocytes. *Am. J. Physiol.* 272:C1594–C1601.

Irons, C.E., C.A. Sei, and C.C. Glembotski. 1993. Regulated secretion of atrial natriuretic factor from cultured ventricular myocytes. *Am. J. Physiol.* 264: H282–H285.

Jiao, J.H., P. Baumann, A. Baron, A. Roatti, R.A. Pence, and A.J. Baertschi. 2000. Sulfonylurea receptor ligands modulate stretch-induced ANF secretion in rat atrial myocyte culture. *Am. J. Physiol. Heart Circ. Physiol.* 278:H2028–H2038.

Krengel, U., L. Schlichting, A. Scherer, R. Schumann, M. Frech, J. John, W. Kabsch, E.F. Pai, and A. Wittinghofer. 1990. Three-dimensional structures of

H-ras p21 mutants: molecular basis for their inability to function as signal switch molecules. *Cell.* 62:539–548.

Lee, S.J., Y. Matsuura, S.M. Liu, and M. Stewart. 2005. Structural basis for nuclear import complex dissociation by RanGTP. *Nature.* 435:693–696.

Lopez, M.J., S.K. Wong, I. Kishimoto, S. Dubois, V. Mach, J. Friesen, D.L. Garbers, and A. Beuve. 1995. Salt-resistant hypertension in mice lacking the guanylyl cyclase-A receptor for atrial natriuretic peptide. *Nature.* 378:65–68.

McGrath, M.F., M.L. de Bold, and A.J. de Bold. 2005. The endocrine function of the heart. *Trends Endocrinol. Metab.* 16:469–477.

Melo, L.G., A.T. Veress, U. Ackermann, and H. Sonnenberg. 1998. Chronic regulation of arterial blood pressure by ANP: role of endogenous vasoactive endothelial factors. *Am. J. Physiol.* 275:H1826–H1833.

Moe, G.W. 2005. BNP in the diagnosis and risk stratification of heart failure. *Heart Fail. Monit.* 4:116–122.

Molkentin, J.D., J.R. Lu, C.L. Antos, B. Markham, J. Richardson, J. Robbins, S.R. Grant, and E.N. Olson. 1998. A calcineurin-dependent transcriptional pathway for cardiac hypertrophy. *Cell.* 93:215–228.

Muth, E., W.J. Driscoll, A. Smalstig, G. Goping, and G.P. Mueller. 2004. Proteomic analysis of rat atrial secretory granules: a platform for testable hypotheses. *Biochim. Biophys. Acta.* 1699:263–275.

Nakagawa, O., M. Nakagawa, J.A. Richardson, E.N. Olson, and D. Srivastava. 1999. HRT1, HRT2, and HRT3: a new subclass of bHLH transcription factors marking specific cardiac, somitic, and pharyngeal arch segments. *Dev. Biol.* 216:72–84.

Roos, K.P. 1986. Length, width, and volume changes in osmotically stressed myocytes. *Am. J. Physiol.* 251:H1373–H1378.

Rossetto, O., L. Gorza, G. Schiavo, N. Schiavo, R.H. Scheller, and C. Montecucco. 1996. VAMP/synaptobrevin isoforms 1 and 2 are widely and differentially expressed in nonneuronal tissues. *J. Cell Biol.* 132:167–179.

Ruskoaho, H., H. Leskinen, J. Magga, P. Taskinen, P. Mantymaa, O. Vuolteenaho, and J. Leppaluoto. 1997. Mechanisms of mechanical load-induced atrial natriuretic peptide secretion: role of endothelin, nitric oxide, and angiotensin II. *J. Mol. Med.* 75:876–885.

Rybkin, I.I., D.W. Markham, Z. Yan, R. Bassel-Duby, R.S. Williams, and E.N. Olson. 2003. Conditional expression of SV40 T-antigen in mouse cardiomyocytes facilitates an inducible switch from proliferation to differentiation. *J. Biol. Chem.* 278:15927–15934.

Shirakawa, R., T. Higashi, A. Tabuchi, A. Yoshioka, H. Nishioka, M. Fukuda, T. Kita, and H. Horiuchi. 2004. Munc13-4 is a GTP-Rab27-binding protein regulating dense core granule secretion in platelets. *J. Biol. Chem.* 279:10730–10737.

Silver, M.A. 2006. The natriuretic peptide system: kidney and cardiovascular effects. *Curr. Opin. Nephrol. Hypertens.* 15:14–21.

Song, K., J. Backs, J. McAnally, X. Qi, R.D. Gerard, J.A. Richardson, J.A. Hill, R. Bassel-Duby, and E.N. Olson. 2006. The transcriptional coactivator CAMTA2 stimulates cardiac growth by opposing class II histone deacetylases. *Cell.* 125:453–466.

Speidel, D., F. Varoqueaux, C. Enk, M. Nojiri, R.N. Grishanin, T.F. Martin, K. Hofmann, N. Brose, and K. Reim. 2003. A family of Ca2+-dependent activator proteins for secretion: comparative analysis of structure, expression, localization, and function. *J. Biol. Chem.* 278:52802–52809.

Speidel, D., C.E. Bruederle, C. Enk, T. Voets, F. Varoqueaux, K. Reim, U. Becherer, F. Fornai, S. Ruggieri, Y. Holighaus, et al. 2005. CAPS1 regulates catecholamine loading of large dense-core vesicles. *Neuron.* 46:75–88.

Sprang, S.R. 1997. G protein mechanisms: insights from structural analysis. *Annu. Rev. Biochem.* 66:639–678.

Sudhof, T.C. 2005. CAPS in search of a lost function. *Neuron.* 46:2–4.

Tamura, N., Y. Ogawa, H. Chusho, K. Nakamura, K. Nakao, M. Suda, M. Kasahara, R. Hashimoto, G. Katsuura, M. Mukoyama, et al. 2000. Cardiac fibrosis in mice lacking brain natriuretic peptide. *Proc. Natl. Acad. Sci. USA.* 97:4239–4244.

Walent, J.H., B.W. Porter, and T.F. Martin. 1992. A novel 145 kd brain cytosolic protein reconstitutes Ca(2+)-regulated secretion in permeable neuroendocrine cells. *Cell.* 70:765–775.

Wennerberg, K., K.L. Rossman, and C.J. Der. 2005. The Ras superfamily at a glance. *J. Cell Sci.* 118:843–846.

Yu, Y., S. Li, X. Xu, Y. Li, K. Guan, E. Arnold, and J. Ding. 2005. Structural basis for the unique biological function of small GTPase RHEB. *J. Biol. Chem.* 280:17093–17100.

Zucman-Rossi, J., P. Legoix, and G. Thomas. 1996. Identification of new members of the Gas2 and Ras families in the 22q12 chromosome region. *Genomics.* 38:247–254.